Terrain correction computation using Gaussian quadrature [☆]

Cheinway Hwang*, Cheng-Gi Wang, Yu-Shen Hsiao

Department of Civil Engineering, National Chiao Tung University, 1001 Ta Hsueh Road, Hsinchu 300, Taiwan

Abstract

A method and a program (tcq) in FORTRAN 90 based on Gaussian quadrature are developed to compute the terrain correction (TC). TCs were determined on 1010 benchmarks using the Gaussian quadrature, prism and FFT methods using a $3'' \times 3''$ elevation grid for the inner zone and a $30'' \times 30''$ elevation grid for the outer zone. In order to achieve a 0.1 mgal accuracy in TC while reducing the computing time, the best inner and outer radii for TC computation are 20 and 200 km, respectively. The Gaussian quadrature is a highly accurate numerical integrator and yields results that outperform those from the prism method and the FFT method. The singular problem of the kernel function in TC is treated by considering the innermost zone effect, which can be expressed as a complete elliptic integral of the first kind. The innermost zone effect must be taken into account if the required accuracy of TC is at a 1-mgal level.
© 2003 Elsevier Ltd. All rights reserved.

Keywords: Gaussian quadrature; Gravity; Innermost zone effect; Taiwan; Terrain correction

1. Introduction

Terrain corrections (TC) are needed in various applications, e.g., geoid computation (Nahavandchi, 2000), interpretation of crustal structure (Camacho et al., 2001) and orthometric correction (Hwang and Hsiao, 2003). Methods for TC computations are abundant in the literature, e.g., Forsberg (1984), Li and Sideris (1994), Nahavandchi and Sjöberg (1998) and Tsoulis (2001). For all these methods, one algorithm is based on the Fast Fourier Transform (FFT) and is suitable for grid-wise computation. The other algorithm is based on the direct integrations of the TC integrals (see later) and is ideal for point-wise computation. In general, the grid-wise algorithm requires less computation time than the point-wise algorithm.

In this paper, a rigorous point-wise method that is based on Gaussian quadrature (e.g., Evans, 1993) will be developed. In TC computation, the singularity in the kernel of integration has been a problem in the past (Forsberg, 1984; Tsoulis, 2001). To account for this singular problem, a method to compute the innermost zone effect (IZE) will be presented. The Gaussian quadrature method will be used to compute TCs on the first-order benchmarks in Taiwan using a high-resolution digital terrain model (DTM), on a $3'' \times 3''$ grid (about 80 m in horizontal resolution).

2. Terrain correction methods

2.1. Direct integration using Gaussian quadrature

In planar approximation, the potential due to the topographic mass above and below a point at (x_P, y_P, s) is (Fig. 1)

$$V = G\rho \int_x \int_y \int_{z=h_p}^{h} \times \frac{\mathrm{d}x\,\mathrm{d}y\,\mathrm{d}z}{\sqrt{(x-x_p)^2 + (y-y_p)^2 + (z-s)^2}}, \quad (1)$$

*Corresponding author. Tel.: +886-3-5724739; fax: +886-3-5716257.

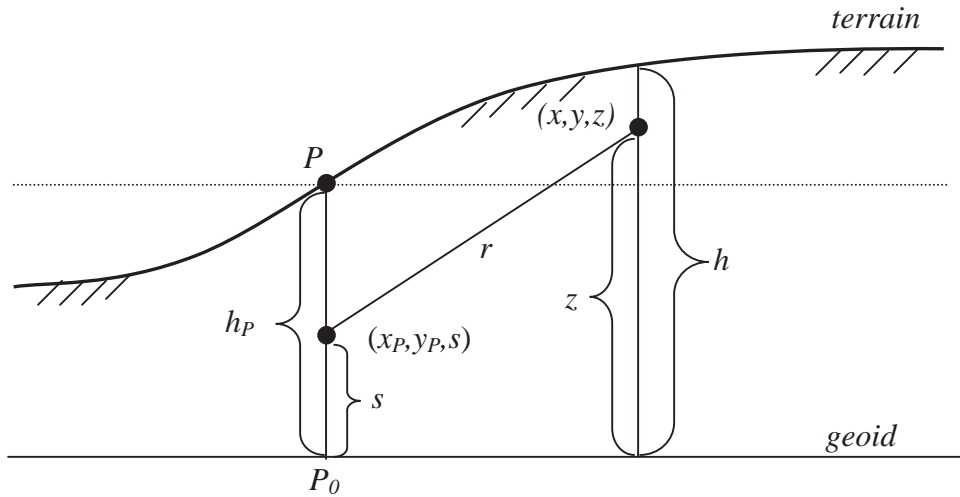*E-mail address:* hwang@geodesy.cv.nctu.edu.tw (C. Hwang).

Fig. 1. Geometry of terrain correction.

where G is the gravitational constant and ρ is the density, which is assumed to be a constant. The vertical component of the attraction, resulting from the potential (Eq. (1)), is called TC expressed at point P as

$$
\begin{aligned}
TC &= \left(\frac{\partial V}{\partial s}\right)\Big|_{s=h_P} = G\rho \int_x \int_y \int_{z=h_P}^{h} \\
&\quad \times \frac{(z-h_P)\,\mathrm{d}x\,\mathrm{d}y\,\mathrm{d}z}{[(x-x_P)^2+(y-y_P)^2+(z-h_P)^2]^{3/2}} \\
&= G\rho \int_x \int_y \left[\frac{1}{\sqrt{(x-x_P)^2+(y-y_P)^2}} \right. \\
&\quad \left. - \frac{1}{\sqrt{(x-x_P)^2+(y-y_P)^2+(h-h_P)^2}} \right] \mathrm{d}x\,\mathrm{d}y \\
&= G\rho \int_x \int_y f(x,y)\,\mathrm{d}x\,\mathrm{d}y. \qquad (2)
\end{aligned}
$$

For a given area bounded by the Cartesian coordinates X_1 (west), X_2 (east), Y_1 (south) and Y_2 (north), Eq. (2) can be evaluated numerically by

$$
\begin{aligned}
TC &= G\rho \int_{X_1}^{X_2} \int_{Y_1}^{Y_2} f(x,y)\,\mathrm{d}x\,\mathrm{d}y \\
&\approx G\rho \sum_{j=1}^{M} w_j^y c(y_j), \qquad (3)
\end{aligned}
$$

where

$$
c(y) = \int_{X_1}^{X_2} f(x,y)\,\mathrm{d}x \approx \sum_{i=1}^{N} w_i^x f(x_i, y), \qquad (4)
$$

where w_i^x and w_j^y are weighting coefficients, x_i and y_j are nodal coordinates, M and N are the numbers of weighting coefficients and nodes along the x and y axes over the domains $[X_1, X_2]$ and $[Y_1, Y_2]$. To achieve the highest possible precision, M and N should be the numbers of the given grids along x and y. Since the DTM in this paper is given on a regular geographic grid, the function values $c(y)$ and $f(x,y)$ at the nodes x_i and y_j were interpolated using the Newton–Gregory forward polynomial (Gerald and Wheatley, 1994) from the evenly spaced function values on a given grid. In the situation of equally spaced data, interpolations based on the Newton–Gregory forward polynomial can be easily programmed and a high interpolation can be achieved, e.g., Hwang and Lin (1998). For the interpolations needed in Eqs. (3) and (4), we have experimented with various polynomial degrees and found that the use of degrees higher than six yields no further improvement in the interpolation accuracy. In our TC program, the subroutine GAULEG from Press et al. (1989), which is designed for the one-dimensional situation, was used successively for the two-dimensional Gaussian quadrature required in Eqs. (3) and (4). The weighting coefficients in the Gaussian quadrature are of the Gauss–Legendre type, as described in standard text books of numerical analysis such as Gerald and Wheatley (1994). With the Gauss–Legendre quadrature, a simple method discussed by Press et al. (1989, p. 125), can be used to compute the weighting coefficients.

Consider the complete elliptic integral of the first kind (Lebedev, 1972)

$$
K(a) = \int_0^{\pi/2} \frac{\mathrm{d}\phi}{\sqrt{1-a^2 \sin^2 \phi}}. \qquad (5)
$$

This function will be used in computing the innermost zone effect of TC, as will be shown later. Fig. 2 shows the relative error using different number of nodes and different values of a. The relative error is defined as the ratio between the absolute error (the absolute difference
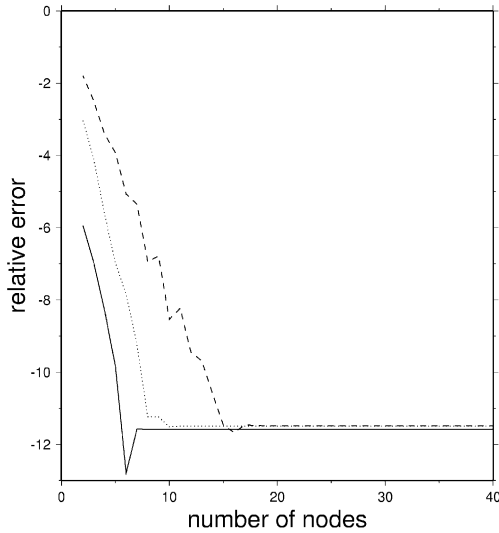
Fig. 2. Relative error (in $\log_{10}$ scale) in using Gaussian quadrature for integrating complete elliptic function, with different a values (see Eq. (5)). (Solid line: $a = 0.1$, dotted line: $a = 0.5$, dashed line: $a = 0.9$).

between the exact value and the approximated value) and the exact value, the latter being computed using the FORTRAN subroutine "CEL" (Press et al., 1989). The relative error increases with a when the number of nodes is below 15, beyond which the relative error is about 10^{-12} irrespective of the number of nodes. This example shows that the Gaussian quadrature method can achieve high accuracy in numerically integrating functions even with a small number of nodes.

2.2. The prism and FFT methods

For comparison, the prism method and the Fourier Transform (FT) method were also used for TC computations. In the prism method, the terrain effect at P (also the origin) due to a rectangular prism bounded by $[x_1, x_2], [y_1, y_2], [z_1, z_2]$ is given by (Forsberg, 1984):

$$C_P = G\rho \left| \left| \left| x \ln(y + r) + y \ln(x - r) \right. \right. \right.$$
$$\left. \left. \left. - z \tan^{-1}\left(\frac{xy}{zr}\right) \right|_{x_1}^{x_2} \right|_{y_1}^{y_2} \right|_{z_1}^{z_2}, \tag{6}$$

where x and y are the horizontal coordinate components, z is the vertical coordinate (also elevation in this case), and $r = \sqrt{x^2 + y^2 + z^2}$. The total terrain effect, or TC, is obtained by summing the contributions from all such prisms. In this paper, the program "tc" authored by Forsberg (1984) was used to compute TCs using the prism method. For the FFT method used in this paper,

a truncated Taylor's expansion of the kernel function in Eq. (2) is used by Forsberg (1984) and leads to the TC at point P as

$$C_P = \tfrac{1}{2} G\rho[l*h^2 - h_P(l*h) + h_P^2 g]$$
$$= \tfrac{1}{2} G\rho \mathbf{F}^{-1}[\mathbf{F}(l)\mathbf{F}(h^2)] - 2h_P \mathbf{F}^{-1}[\mathbf{F}(l)\mathbf{F}(h)]$$
$$+ h_P^2 \mathbf{F}^{-1}[L(0,0)], \tag{7}$$

where

$$l(x, y) = \frac{1}{(x^2 + y^2)^{3/2}}, \quad g = \int \int l \, \mathrm{d}x \, \mathrm{d}y. \tag{8}$$

$\mathbf{F}$ and $\mathbf{F}^{-1}$ are the direct and inverse FT operators, respectively, and $L(0, 0)$ is the FT of l at frequency zero. The convolutions in Eq. (7) can be carried out using FFT to achieve high computational efficiency. In this paper, Eq. (7) is implemented by program "tcfour", also developed by Forsberg (1984). Note that Eq. (7) is only one approximation of the rigorous FFT methods for TC computations. TC computations by FFT with more rigorous formulae are given by Li and Sideris (1994) and Tsoulis (2001).

3. The innermost zone effect

The kernel function $f(x, y)$ in Eq. (2) is singular at the computational point p, i.e., $x = x_p, y = y_p$. This singular problem has been discussed by Schwarz et al. (1990), Bian and Sun (1994), and Tsoulis (2001). Here we present a solution using a method similar to the method for evaluating the innermost zone effect in Stokes' integral (Heiskanen and Moritz, 1967). In Eq. (2), the elevation near P can be expanded in a Taylor series

$$h = h_P + xh_x + yh_y + \tfrac{1}{2}(x^2 h_{xx} + xy h_{xy} + y^2 h_{yy}) + \cdots, \tag{9}$$

where

$$h_x = \frac{\partial h}{\partial x}, \quad h_y = \frac{\partial h}{\partial y}, \quad h_{xx} = \frac{\partial^2 h}{\partial x^2},$$
$$h_{xy} = \frac{\partial^2 h}{\partial x \partial y}, \quad h_{yy} = \frac{\partial^2 h}{\partial y^2}. \tag{10}$$

Restricting the Taylor series to the linear term only and using polar coordinates, the contribution from the topographic mass within the innermost zone, which is defined as a circle of radius s_0 around P, is (see Eq. (2))

$$C_i = G\rho \int_{s=0}^{s_0} \int_{\alpha=0}^{2\pi} \frac{1}{r} r \, \mathrm{d}s \, \mathrm{d}\alpha$$
$$- G\rho \int_{s=0}^{s_0} \int_{\alpha=0}^{2\pi} \frac{1}{[r^2 + (rh_x \sin\alpha + rh_y \cos\alpha)^2]^{1/2}}$$
$$\times r \, \mathrm{d}s \, \mathrm{d}\alpha = A - B. \tag{11}$$

Evaluating the integrals, the A term is

$$A = 2\pi G\rho s_0, \tag{12}$$

and the B term is

$$
\begin{aligned}
B &= G\rho s_0 \int_0^{2\pi} \frac{1}{[1 + (h_x \sin\alpha + h_y \cos\alpha)^2]^{1/2}} \, d\alpha \\
&= G\rho s_0 \int_0^{2\pi} \frac{1}{(1 + a^2 \sin^2\theta)^{1/2}} \, d\theta \\
&= 4G\rho s_0 \frac{1}{\sqrt{1 + a^2}} \int_0^{\pi/2} \frac{1}{\sqrt{1 - \frac{a^2}{1+a^2}\sin^2\theta}} \, d\theta \\
&= 4G\rho s_0 \frac{1}{\sqrt{1 + a^2}} K\left(\frac{a}{\sqrt{1 + a^2}}\right),
\end{aligned} \tag{13}
$$

where K is the complete elliptic integral of the first kind defined in Eq. (5), and a is the gradient of terrain defined as

$$
a = \sqrt{h_x^2 + h_y^2}. \tag{14}
$$

If the elevation data are given on a regular geographic grid with intervals $\Delta\phi$ and $\Delta\lambda$ in latitude and longitude, the radius of the innermost zone can be approximated by

$$
s_0 \approx R\sqrt{\frac{\cos\phi \, \Delta\phi \, \Delta\lambda}{\pi}}, \tag{15}
$$

where R is the mean Earth radius (≈ 6371 km) and ϕ is latitude.

4. Results

4.1. Result from tcq: a program based on Gaussian quadrature

The gravity values were collected on 1010 first-order benchmarks, where TCs are to be applied. For TC computations on these benchmarks, two elevation data sets were used: one data set is on a $3'' \times 3''$ grid and the other is on a $30'' \times 30''$ grid. These grids were generated by Hwang and Hsiao (2003) using a total of 6 421 075 point elevation data in Taiwan, covering the area over $21.5°$–$25.5°$N and $119.5°$–$122.5°$E. Fig. 3 shows a shaded relief map of the terrain and the distribution of the 1010 benchmarks. The terrain over Taiwan is complex and contains plains, foothills and alpine mountains. The highest point is in the Central Range, reaching 3952 m. In Eastern Taiwan, mountains can be as high as 2000 m only several km from the coast, creating large terrain effects for benchmarks situated on coastal highways.

Because computation by the Gaussian quadrature method for TC is relatively time consuming as compared to the FFT method, the best computational strategy is to split the TC into two parts: the inner zone with a fine elevation grid and the outer zone with a coarse elevation grid, (see Fig. 4). Such a strategy was recommended by
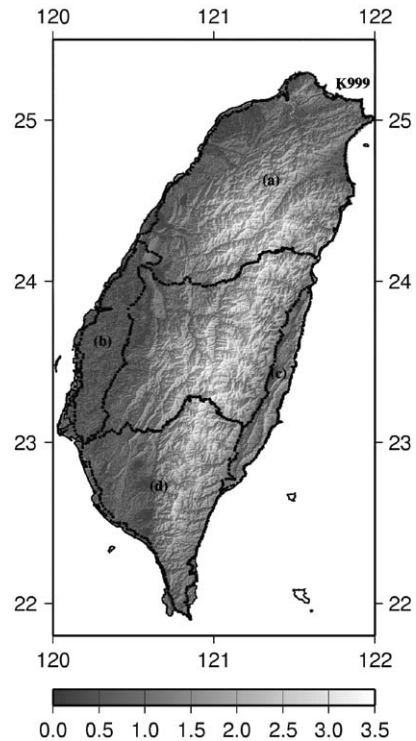

Fig. 3. Shaded relief map of terrain in Taiwan and 1010 benchmarks (black dots) where terrain corrections are to be computed.
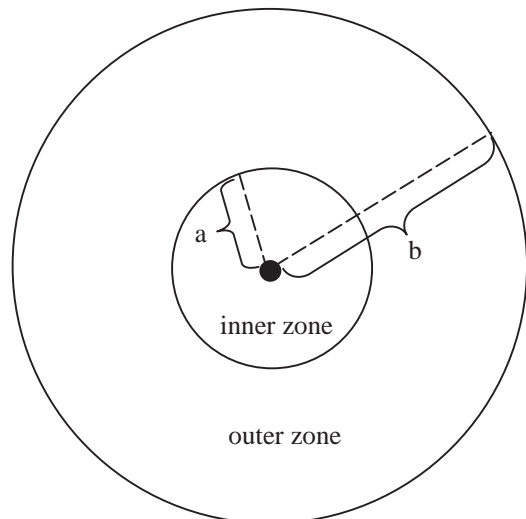

Fig. 4. Division of computation for terrain correction. Black circle is innermost zone, a and b are radii of inner and outer zones, respectively.

Forsberg (1984). Based on this strategy, a program "tcq" in FORTRAN 90 was developed. Program tcq also computes the innermost zone effect using

Eq. (11) with the radius given by Eq. (15). In this paper, the $3'' \times 3''$ grid was used for the effect of the inner zone, and the $30'' \times 30''$ grid was used for the effect of the outer zone. The gradients of the terrain needed in the innermost zone effect are obtained by first fitting polynomials to a window of 20×20 gridded elevations surrounding the computation point, and then evaluating the gradients using the fitted polynomials. The IMSL subroutine DQD2DR was used for polynomial fitting and gradient evaluation.

To save computing time, it is necessary to find the smallest radii of the inner and outer zones (hereafter called inner radius and outer radius) that will still meet the accuracy requirement of TC. (Note that the choice of radii will also depend on the roughness of the terrain under study). To see how the inner radius affects the TC, differences between the TCs from using two different inner radii were determined and are shown in Fig. 5. From Fig. 5, the maximum difference in TC decreases as the inner radius increases. The maximum differences in TC for the inner radii of 2–5, 5–10, 10–15, 15–20, 20–30, 30–40, 40–50, and 50–60 km are 1.7, 1.02, 0.46, 0.18, 0.09, 0.07, 0.12, and 0.04 mgal, respectively. Based on these statistics and Fig. 5, it is concluded that, if the
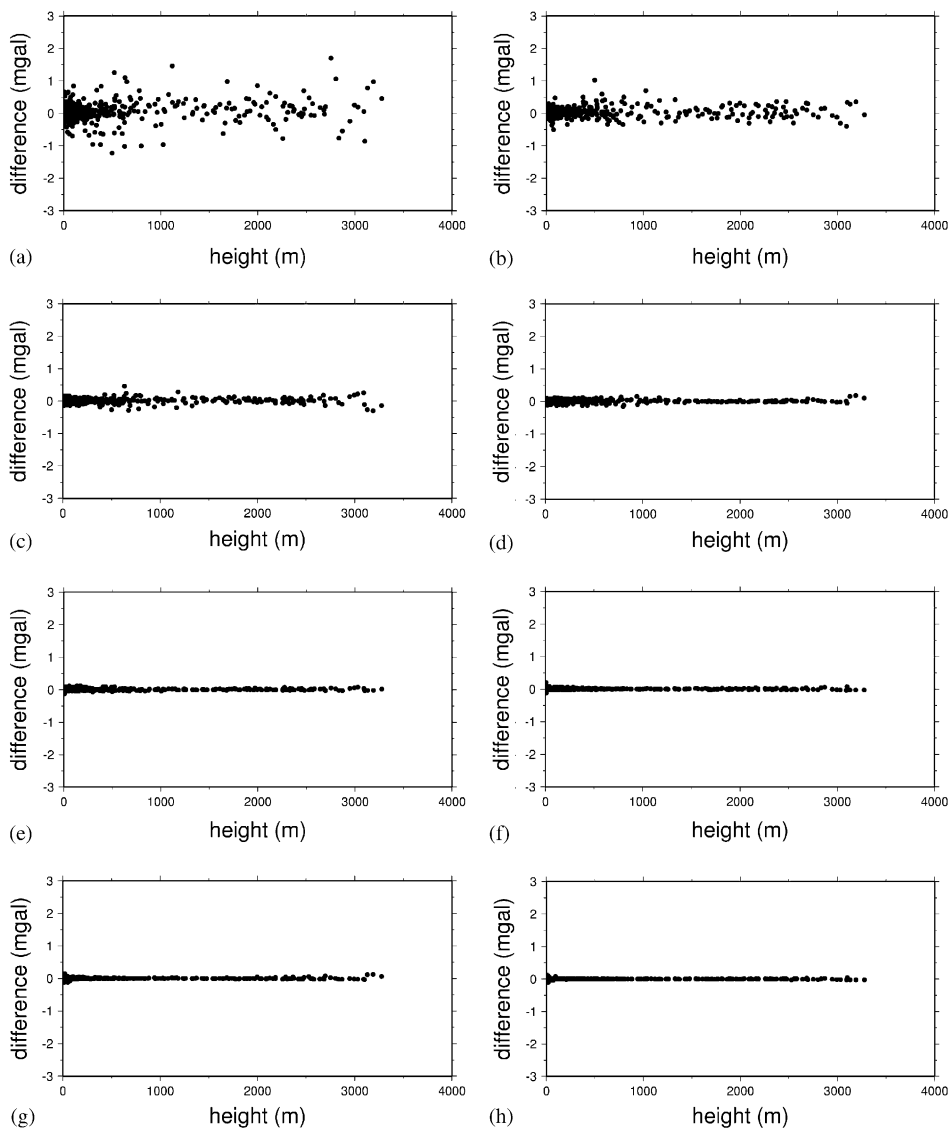

Fig. 5. Difference in terrain correction using two different radii (in km) of inner zone: (a) 5 and 2, (b) 10 and 5, (c) 15 and 10, (d) 20 and 15, (e) 30 and 20, (f) 40 and 30, (g) 50 and 40, (h) 60 and 50. A radius of 400 km for outer zone is used.

required accuracy of TC is 0.1 mgal, an inner radius of 20 km is sufficient.

It is also important to determine the smallest outer radius beyond which the terrain effect can be neglected. Fig. 6 shows the differences in TC from using two different outer radii. The maximum differences in TC for the outer radii of 100–400, 150–400, 200–400, and 300–400 km are 2.31, 0.62, 0.17, and 0.10 mgal, respectively. In the cases of 100–400 and 150–400 km, the difference increases with elevation. Thus, to meet a 0.1-mgal accuracy in TC, an outer radius of 200 km will be sufficient. Also, at elevations less than 1000 m, the differences in TC from using a radius of 100 km and a radius of 400 km are less than 0.1 mgal, and this shows that an outer radius of 100 km is sufficient for TCs at elevations below 1000 m.

Using an inner radius of 20 km and an outer radius of 200 km, the TCs at the 1010 benchmarks (Fig. 3) were computed and the result is given in Fig. 7. The maximum, minimum, mean and standard deviation of the TCs are 85.53, 0.36, 10.08, and 13.74 mgal, respectively. The largest TC (85.53 mgal) occurs at a benchmark where the elevation is 3500 m. In general, the TC value increases with elevation. However, large
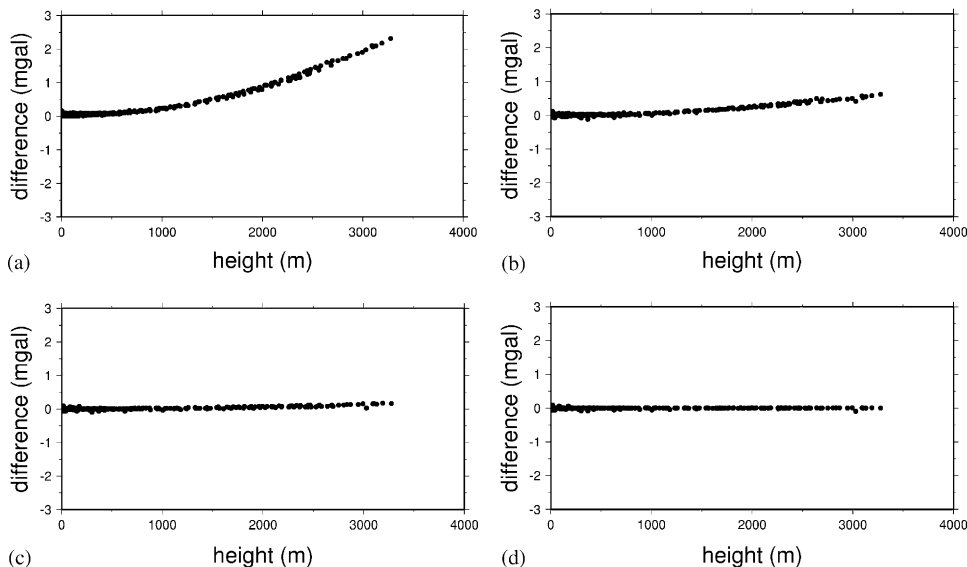

Fig. 6. Difference in terrain correction using two different radii (in km) of outer zone: (a) 400 and 100, (b) 400 and 150, (c) 400 and 200, (d) 400 and 300. A radius of 20 km for inner zone is used.
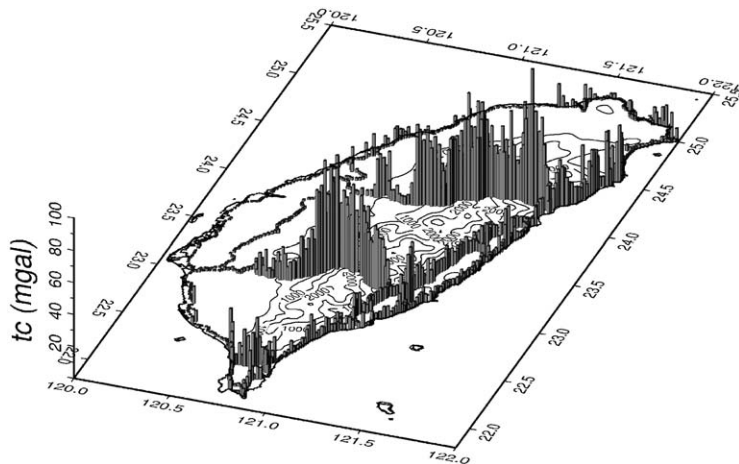

Fig. 7. Terrain corrections using Gaussian quadrature method on 1010 benchmarks using an inner radius of 20 km and an outer radius of 200 km.

TC values also exist near the coastal highway in northeastern Taiwan, where the elevations are low. These large TCs are caused by the high mountains (over 2000 m) on the western flank of this highway. In addition, Fig. 8 shows the computing times using different inner and outer radii on a Pentium 4 machine with a clock rate of 2 GHz. The computing time is mainly governed by the inner radius and it increases nonlinearly with the inner radius. The outer radius also affects the computing time. The computing time for a 400-km outer radius is 250 CPU seconds more than that for a 100-km outer radius.

Fig. 9 shows the innermost zone effects at the 1010 benchmarks. The maximum, minimum, mean and standard deviation of the innermost zone effect are 1.71, 0.00, 0.10 and 0.24 mgal, respectively. Thus, in order to achieve a 1-mgal accuracy in TC, the innermost zone effect must be taken into account. Furthermore, it can be shown that the B term in Eq. (13) decreases with an increasing gradient of terrain. As a result, the innermost zone effect (Eq. (11) increases with gradient. In general, the gradient increases with the elevation
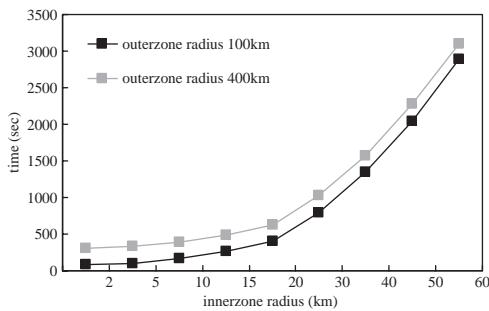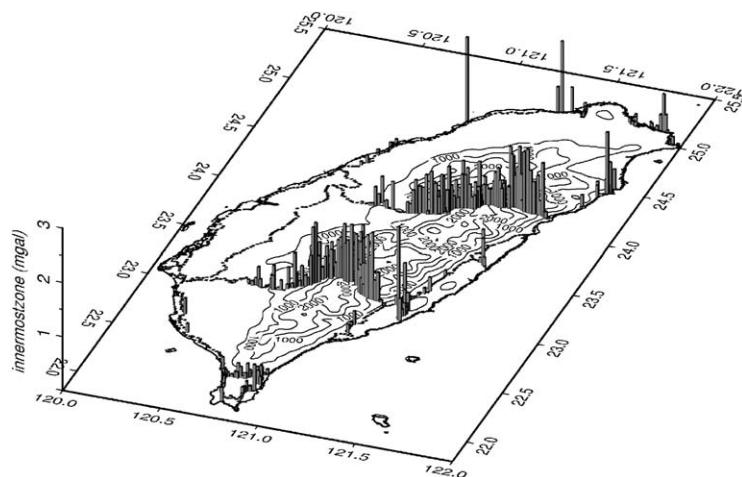
(Fig. 3), thus the innermost zone effect also increases with elevation (the correlation coefficient between the two is 0.6). However, large innermost zone effects also exist at some benchmarks with low elevations along the coastal highway in northeastern Taiwan. This is, again, due to the special condition of the terrain here as already mentioned.

4.2. Comparison among TCs from Gaussian quadrature, prism and FFT methods

TCs using the prism and the FFT methods were also determined on the 1010 benchmarks. These two methods are implemented by programs ''tc'' and ''tcfour'' provided by Forsberg (1984). Programs tc and tcfour, like tcq, also divide the TC computation into an inner zone and an outer zone, but they do not take into account the innermost zone effect. In fact, for these two methods, TCs were first determined on the same $3'' \times 3''$ grid as the elevation grid, and the TCs on the benchmarks were then obtained by interpolations using the Newton–Gregory polynomial. Fig. 10a shows the TCs from the prism method (Eq. (6)) and Fig. 10b the TCs from the FFT method (Eq. (7)). Table 1 shows the statistics of the TCs from these three methods. Table 2 shows the statistics of the differences in TC from the three methods. As shown in Fig. 10 and Table 1, the Gaussian quadrature method picks up more high-frequency variations in TC than do the other two methods. The FFT method delivers TCs with the lowest magnitude and resolution. For example, along the coastal highways in western and eastern Taiwan, the FFT method cannot correctly compute the effect of the terrain, whereas the other two methods successfully recover the terrain signals. The 2.31-mgal difference (in standard deviation) between the Gaussian

Fig. 8. Computing times using different inner and outer radii.

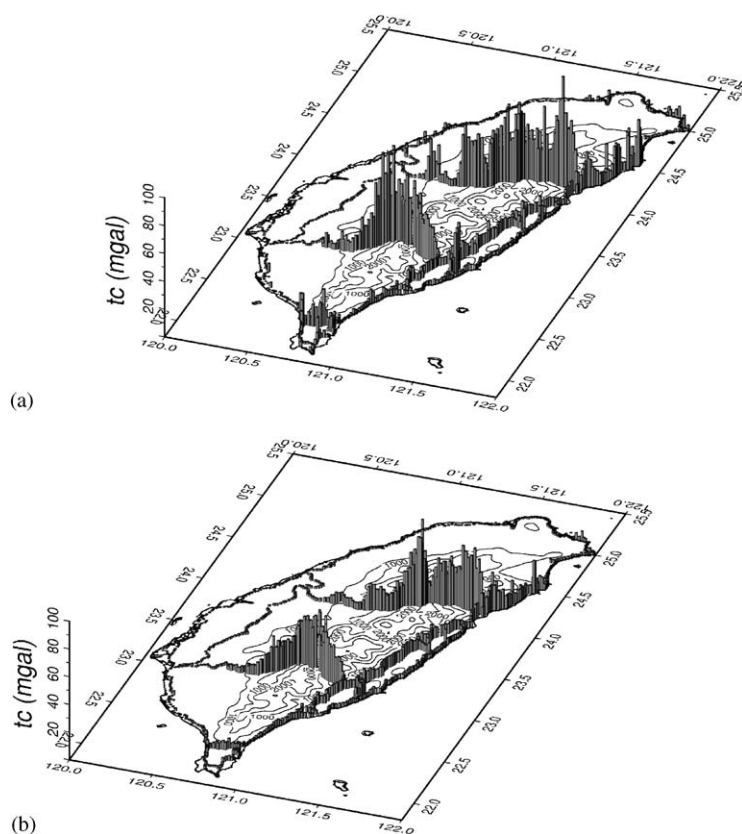Fig. 9. Innermost zone effect on 1010 benchmarks.

Fig. 10. Terrain corrections from (a) prism method and (b) FFT method.

Table 1
Statistics of terrain corrections (in mgal) on 1010 benchmarks from different methods

	Maximum	Minimum	Mean	Std. dev.
Gauss quadrature	85.44	0.25	9.95	13.58
Prism	79.16	0.10	8.30	12.47
FFT	61.86	0.22	6.39	9.21

Table 2
Statistics of differences (in mgal) in terrain corrections from different methods

	Maximum	Minimum	Mean	Std. dev.
Gauss–prism	14.78	−3.94	1.65	2.31
Gauss–FFT	48.89	−25.39	3.56	7.28
Prism–FFT	45.39	−25.19	1.91	6.18

quadrature and the prism methods does not entirely come from the innermost zone effect, and it shows that the prism method may still have room for improvement. Furthermore, Fig. 11 shows the differences among the three methods with respect to elevation. As expected, large differences occur at high elevations, and at low elevations where the terrain is complex (e.g. along the coastal highways).

To compare computing time, TCs on a $1' \times 1'$ grid over the domain $119.5°$–$122.5°$E and $21.5°$–$25.5°$N (total 43 621 points) are determined using the three methods. The required computing times are 30 281 (Gauss quadrature), 6569 (prism) and 3 (FFT) CPU seconds, respectively, on a Pentium 4, 2-GHz clock rate machine. Thus the Gaussian quadrature method is 4.6 times slower than the prism method. However, the Gaussian quadrature method is intended for a point-by-point computation and it would be a waste of computing time to use Gaussian quadrature for a grid-wise computation. In fact, it takes only 701 CPU seconds (on the same machine) to compute the TCs on the 1010 benchmarks by Gaussian quadrature, and the achieved accuracy in TC is worth such a computing time.
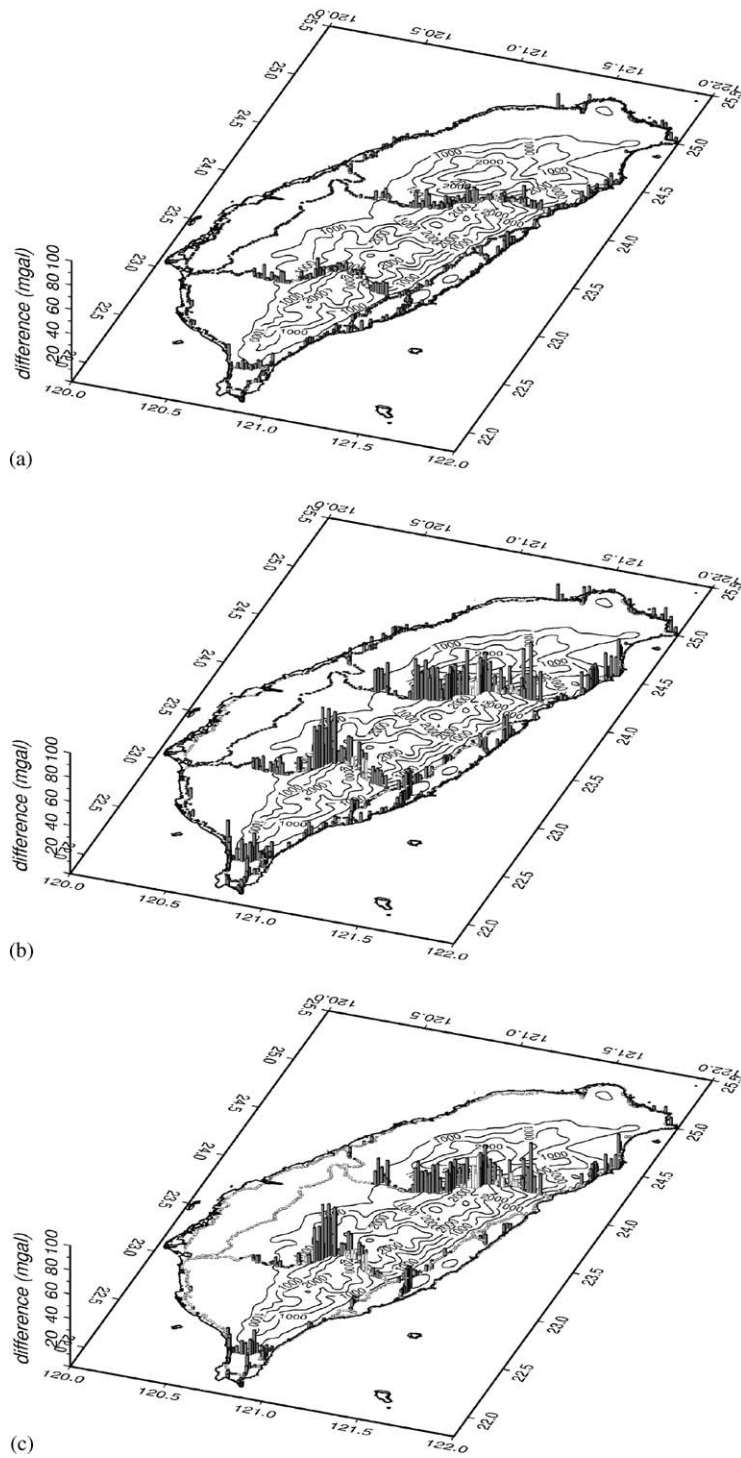
Fig. 11. Differences in terrain correction from using two different methods: (a) Gaussian quadrature and prism (b) Gaussian quadrature and FFT (c) prism and FFT.

5. Conclusions

In this paper, the Gaussian quadrature method is used to compute the TCs on 1010 benchmarks. This method yields improved TCs over the prism method and the approximated FFT method. The Gaussian quadrature method required more computer time than the other two methods, but this does not pose any problem given today's computing environment. Based on a Taylor series expansion, the innermost zone effect was derived; it is approximated by an elliptic integral and a function of the radius of the innermost zone and the gradient of the neighboring terrain. The innermost zone effect over Taiwan must be taken into account if the required accuracy of TC is at a 1-mgal level. The program tcq that computes TCs using the Gaussian quadrature method is available from the authors, or may be downloaded from the IAMG server.

Acknowledgements

References

Bian, S., Sun, H., 1994. The expression of common singular integrals in physical geodesy. Manuscripta Geodaetica 19, 62–69.

Camacho, A.G., Montesinos, F.G., Vieira, R., Arnoso, J., 2001. Modelling of crustal anomalies of Lanzarote (Canary Islands) in light of gravity data. Geophysical Journal International 147, 403–414.

Evans, G., 1993. Practical Numerical Integration. Wiley, New York, 328pp.

Forsberg, R., 1984. A study of terrain reductions, density anomalies and geophysical inversion methods in gravity field modeling. Report no 355, Department of Geodesic Science and Survey, Ohio State University, Columbus, OH, 129pp.

Gerald, C.F., Wheatley, P.O., 1994. Applied Numerical Analysis, 5th Edition. Addison Wesley Publication Co, New York, 748pp.

Heiskanen, W.A., Moritz, H., 1967. Physical Geodesy. WH Freeman and Co, San Francisco, 364pp.

Hwang, C., Hsiao, Y.S., 2003. Orthometric corrections from leveling, gravity, density and elevation data: a case study in Taiwan. Journal of Geodesy 77, 279–291.

Hwang, C., Lin, M.-J., 1998. Fast integration of low orbiter's trajectory perturbed by earth's nonsphericity. Journal of Geodesy 72, 578–585.

Lebedev, N.N., 1972. Special Functions and their Applications. Dover Publication, New York, 308pp.

Li, Y.C., Sideris, M., 1994. Improved gravimetric terrain correction. Geophysical Journal International 119, 740–752.

Nahavandchi, H., 2000. The direct topographical correction in gravimetric geoid determination by the Stokes-Helmert method. Journal of Geodesy 74, 488–496.

Nahavandchi, H., Sjöberg, L., 1998. Terrain correction to the power H^3 in gravimetric geoid determination. Journal of Geodesy 72, 124–135.

Press, W.H., Flannery, B.P., Teukolsky, S.A., Vetterling, W.T., 1989. Numerical Recipes. Cambridge University Press, New York, 874pp.

Schwarz, K.P., Sideris, M., Forsberg, R., 1990. The use of FFT techniques in physical geodesy. Geophysical Journal International 100, 485–514.

Tsoulis, D., 2001. Terrain correction computations for a densely sampled DTM in the Bavarian Alps. Journal of Geodesy 75, 291–307.